

Influence of lipid bilayer properties on nanodisc formation mediated by styrene/maleic acid copolymers

Electronic Supplementary Information (ESI)

Rodrigo Cuevas Arenas, Johannes Klingler, Carolyn Vargas, and Sandro Keller*

Molecular Biophysics
University of Kaiserslautern
Erwin-Schrödinger-Str. 13
67663 Kaiserslautern
Germany

*mail@sandrokeller.com

Theoretical Background	1
Data Analysis	2
Supplementary Figures.....	4
Supplementary Table.....	6
Supplementary References	7

Theoretical Background

Pseudophases in lipid/polymer mixtures

We have shown¹ that the solubilisation of POPC membranes by SMA(3:1) copolymers can be rationalised within the three-stage model,² which considers lipid (L) and surfactant (S) molecules in the bilayer (b) and the micellar (m) phases as well as, in the general case, surfactant monomers in the aqueous phase (aq). The concentrations of lipid (c_L) and surfactant (c_S) determine the presence and abundance of each of these phases. In a lipid/polymer mixture, where the polymer takes the role of the surfactant, an increase in c_S at given c_L leads to a transition from the vesicular bilayer range to the coexistence range, where polymer-saturated bilayer vesicles coexist with lipid-saturated nanodiscs called SMALPs. Upon a further increase in c_S , the vesicles are completely solubilised and transformed into SMALPs. In this interpretation of the three-stage model, SMALPs are equivalent to mixed micelles found in conventional lipid/surfactant mixtures. The first SMALPs are formed at a threshold known as the saturation (SAT) boundary, while a second transition designated as the solubilisation (SOL) boundary marks the completion of SMALP formation and the concomitant disappearance of the last vesicular structures.

Plotting the c_S values at the SAT and SOL boundaries, c_S^{SAT} and c_S^{SOL} , respectively, against c_L results in two straight lines described by:

$$c_S^{\text{SAT}} = c_S^{\text{aq},0} + R_S^{\text{b,SAT}} c_L \quad (1)$$

$$c_S^{\text{SOL}} = c_S^{\text{aq},0} + R_S^{\text{m,SOL}} c_L \quad (2)$$

where $R_S^{\text{b,SAT}}$ and $R_S^{\text{m,SOL}}$ denote the polymer/lipid molar ratios in vesicular bilayers and SMALPs at which the membrane becomes saturated with polymer and at which solubilisation is complete, respectively. $c_S^{\text{aq},0}$ is the concentration of “free” polymer in the aqueous phase within the coexistence range. In both our previous¹ and present phase diagrams (*cf.* Fig. 1c, Fig. 3c, and Fig. 4c), the ordinate intercepts of the SAT and SOL boundaries were negligibly low, so that the concentration of SMA(3:1) in the aqueous phase was taken as $c_S^{\text{aq},0} = 0$.

The saturating and solubilising mole fractions of polymer in bilayer vesicles and SMALPs, $X_S^{\text{b,SAT}}$ and $X_S^{\text{m,SOL}}$, respectively, are calculated from the corresponding molar ratios as:

$$X_S^{\text{b,SAT}} = \frac{R_S^{\text{b,SAT}}}{1 + R_S^{\text{b,SAT}}} \quad (3)$$

$$X_S^{\text{m,SOL}} = \frac{R_S^{\text{m,SOL}}}{1 + R_S^{\text{m,SOL}}} \quad (4)$$

The partition coefficients quantifying the transfer of polymer and lipid from vesicular bilayers into SMALPs, $K_S^{\text{b} \rightarrow \text{m}}$ and $K_L^{\text{b} \rightarrow \text{m}}$, are then given by:

$$K_S^{\text{b} \rightarrow \text{m}} \equiv \frac{X_S^{\text{m,SOL}}}{X_S^{\text{b,SAT}}} = \frac{R_S^{\text{m,SOL}}(1 + R_S^{\text{b,SAT}})}{R_S^{\text{b,SAT}}(1 + R_S^{\text{m,SOL}})} > 1 \quad (5)$$

$$K_L^{\text{b} \rightarrow \text{m}} \equiv \frac{X_L^{\text{m,SOL}}}{X_L^{\text{b,SAT}}} = \frac{1 - X_S^{\text{m,SOL}}}{1 - X_S^{\text{b,SAT}}} = \frac{1 + R_S^{\text{b,SAT}}}{1 + R_S^{\text{m,SOL}}} < 1 \quad (6)$$

From these partition coefficients, the corresponding standard molar Gibbs free-energy changes accompanying the transfer of the polymer and the lipid from bilayer vesicles into SMALPs, $\Delta G_S^{\text{b} \rightarrow \text{m},0}$ and $\Delta G_L^{\text{b} \rightarrow \text{m},0}$, respectively, are obtained as:

$$\Delta G_S^{b \rightarrow m, o} = -RT \ln K_S^{b \rightarrow m} < 0 \quad (7)$$

$$\Delta G_L^{b \rightarrow m, o} = -RT \ln K_L^{b \rightarrow m} > 0 \quad (8)$$

Data Analysis

Best-fit parameter values and 95% confidence intervals were derived by nonlinear least-squares fitting in Excel spreadsheets, as detailed elsewhere.³

Derivation of phase boundaries from ³¹P NMR data

According to the three-stage model, all phospholipid molecules reside in lipid bilayers as long as the polymer concentration is lower than or equal to c_S^{SAT} (eqn (1)). In solution-state NMR experiments employing relatively narrow sweep widths, the signal arising from ³¹P nuclei in large, vesicular structures is broadened beyond detection.^{1,4-6} Thus, the area of the ³¹P NMR peak, A , is zero in the absence of solubilised phospholipid:

$$A(c_S \leq c_S^{\text{SAT}}) = 0 \quad (9)$$

Once the polymer concentration reaches or exceeds c_S^{SOL} (eqn (2)), all phospholipid molecules are solubilised in SMALPs, resulting in a sharp, isotropic NMR signal whose area amounts to:

$$A(c_S^{\text{SOL}} \leq c_S) = f c_L \quad (10)$$

where the proportionality factor, f , depends on experimental conditions but is constant for a given NMR spectrometer and identical instrument settings and acquisition parameters. Within the coexistence range, the peak area is proportional to the amount of solubilised phospholipid, which is described by:

$$A(c_S^{\text{SAT}} \leq c_S \leq c_S^{\text{SOL}}) = f c_L \frac{c_S - c_S^{\text{b,SAT}}}{c_S^{\text{m,SOL}} - c_S^{\text{b,SAT}}} \quad (11)$$

The peak area can be expressed in terms of $R_S^{\text{b,SAT}}$ and $R_S^{\text{m,SOL}}$ by dividing both the numerator and the denominator in eqn (11) by c_L and considering eqn (1) and (2):

$$A(c_S^{\text{SAT}} \leq c_S \leq c_S^{\text{SOL}}) = f c_L \frac{c_S/c_L - R_S^{\text{b,SAT}}}{R_S^{\text{m,SOL}} - R_S^{\text{b,SAT}}} \quad (12)$$

The terms on the right-hand sides of eqn (11) and (12) reflect the fraction of solubilised lipid as given by the lever rule.^{7,8}

Pairs of $c_S^{\text{b,SAT}}$ and $c_S^{\text{m,SOL}}$ values at a given lipid concentration were obtained by analysing the areas derived from the corresponding ³¹P NMR signals in terms of eqn (9)–(11), as described previously.¹ In addition to such local fits considering only one lipid concentration at a time, peak areas measured at four different lipid concentrations were globally fitted with eqn (9), (10), and (12) in order to obtain the best-fit $R_S^{\text{b,SAT}}$ and $R_S^{\text{m,SOL}}$ values.

Peak fitting of ³¹P NMR spectra

The ³¹P NMR signal arising from solubilised phospholipid molecules displays one or several isotropic, Lorentzian-shaped peaks, with the number of peaks corresponding to the number of distinct chemical environments. Differences among chemical environments may be due to, among other factors, different compositions of the phospholipids themselves^{5,6} but also changes in the phase state of the bilayer in which they reside.^{9,10} To extract the position,

width, and area of a single peak, experimental data were fitted using a Lorentzian function described by:

$$L(\delta) = g \frac{\Gamma/2}{(\delta - \delta_0)^2 + (\Gamma/2)^2} \quad (13)$$

where δ , δ_0 , and Γ are the chemical shift, the chemical-shift position of the peak centre, and the peak width at half-maximal intensity, respectively. The parameter g is a proportionality factor that depends on experimental conditions but is constant for data acquired under identical conditions. The area under the fitted curve—corresponding to the amount of phospholipid solubilised in the form of SMALPs—was determined by integration over all $L(\delta)$ values across the fitted peak range. ^{31}P NMR signals of SMALPs harbouring both POPC and POPE or DMPC in different states (i.e., presumably gel and liquid-crystalline) were analysed in terms of a double-Lorentzian function analogous to that in eqn (13) to extract the peak position, width, and area of either peak individually.

Supplementary Figures

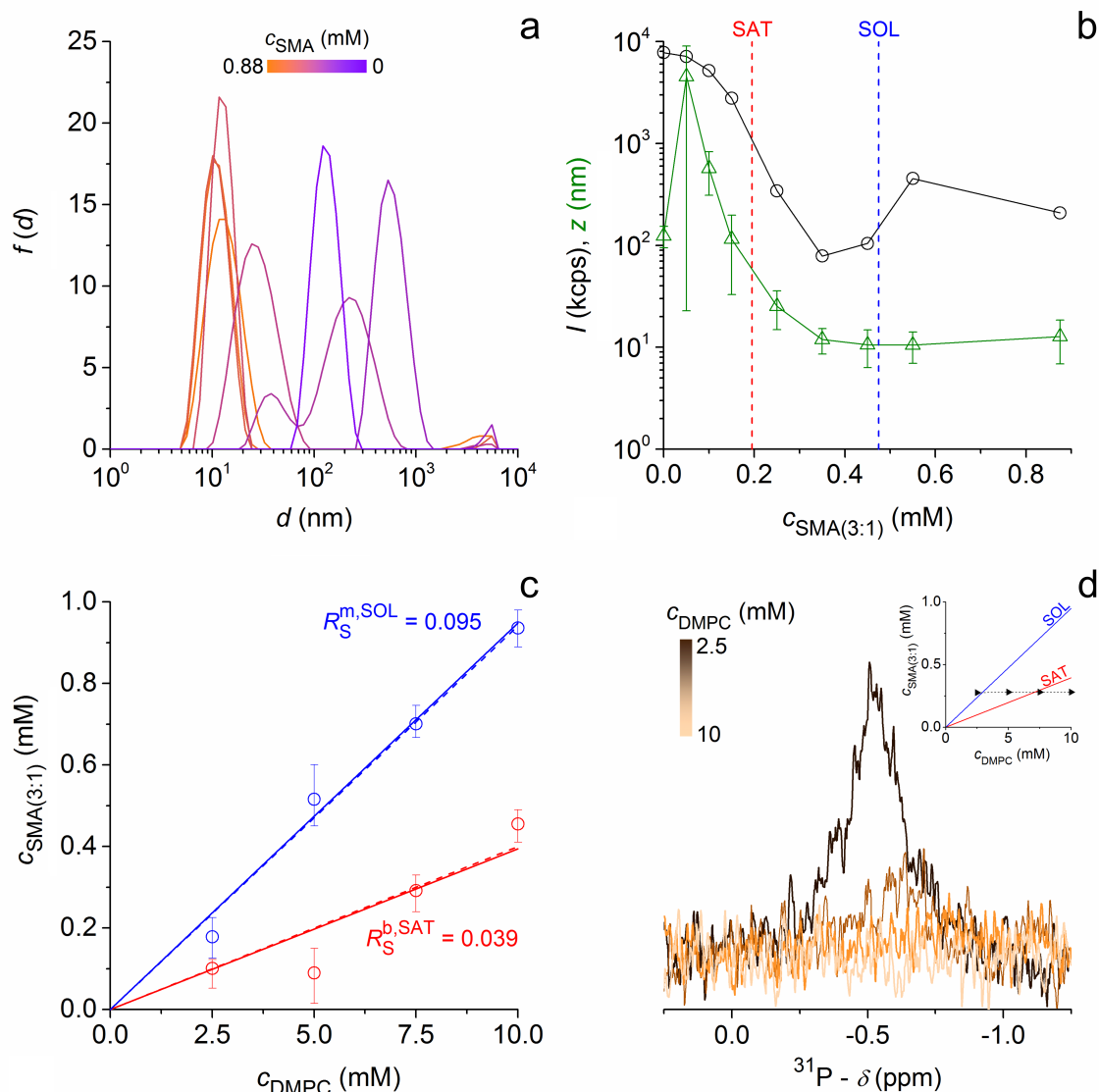


Fig. S1. Solubilisation and reconstitution of gel-phase DMPC vesicles by SMA(3:1) at 10 °C. (a) Intensity-weighted particle size distribution functions, $f(d)$, versus hydrodynamic diameter, d , obtained upon exposure of 5 mM DMPC LUVs to increasing concentrations of SMA(3:1). (b) Total light scattering intensity at 90°, I , and z -average particle diameter, z , as functions of SMA(3:1) concentration. Also indicated are the SAT and SOL boundaries (dashed lines) derived from ^{31}P NMR experiments (Fig. 3). Vertical bars denote peak widths as given by the corresponding PDI values. (c) Phase diagram of DMPC/SMA(3:1) at 10 °C. Pairs of $c_S^{b,\text{SAT}}$ and $c_S^{m,\text{SOL}}$ (circles) obtained from breakpoints derived from local fits according to eqn (9)–(11), linear regressions to these data (dashed lines), and global fits (solid lines) according to eqn (9), (10), and (12) indicating the onset (SAT; red) and completion (SOL; blue) of solubilisation, respectively. Error bars are 95% confidence intervals of local fits based on eqn (9)–(11). (d) NMR spectra of 2.5 mM DMPC and 0.28 mM SMA(3:1) initially present in the form of SMALPs upon addition of DMPC LUVs. Inset: Phase diagram of DMPC/SMA(3:1) at 10 °C indicating the SAT (red) and SOL (blue) boundaries from (c) and the DMPC concentrations tested in the reconstitution assay (triangles).

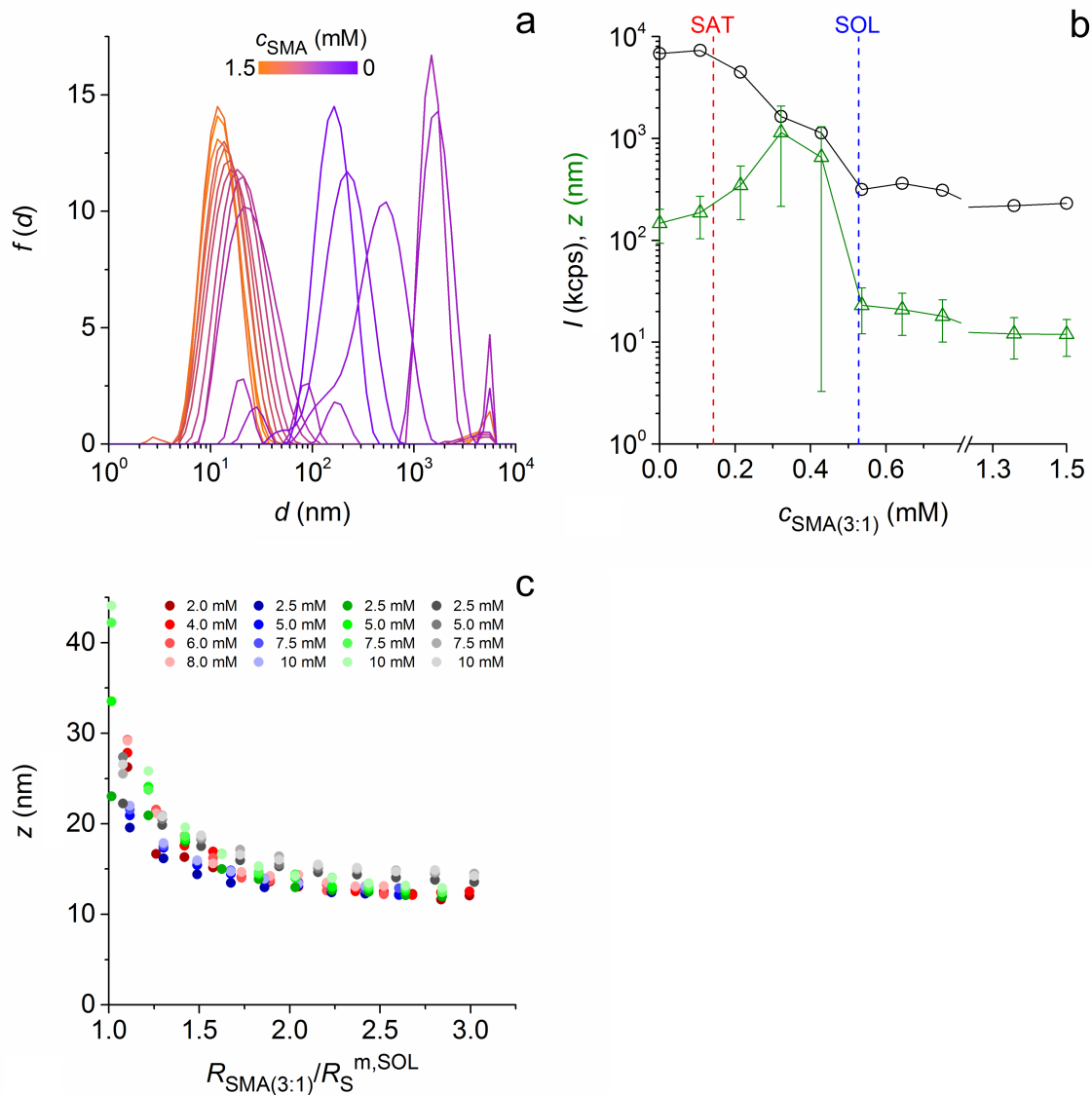


Fig. S2. Solubilisation of POPC/POPE LUVs by SMA(3:1) at 30 °C as monitored by DLS. (a) Intensity-weighted particle size distribution functions, I , versus hydrodynamic diameter, d , obtained upon exposure of 2.5 mM POPC/POPE(1:1) LUVs to increasing concentrations of SMA(3:1). (b) Total light scattering intensity at 90°, I , and z -average particle diameter, z , as functions of SMA(3:1) concentration. Also indicated are the SAT and SOL boundaries (dashed lines) derived from ^{31}P NMR experiments (Fig. 4). Vertical bars denote peak widths as given by the corresponding PDI values. (c) z -average particle diameters, z , at various total lipid concentrations and four different POPC/POPE ratios as functions of the SMA(3:1)/lipid molar ratio, $R_{\text{SMA}(3:1)}$, normalised by the corresponding solubilising molar ratio, $R_{\text{S}}^{\text{m,SOL}}$, as obtained for POPC/POPE(1:0) (red), POPC/POPE(3:1) (blue), POPC/POPE(1:1) (green), and POPC/POPE(1:3) (grey).

Supplementary Table

Table S1. Changes in standard molar Gibbs free energy, $\Delta G^{b \rightarrow m, o}$, accompanying the transfer of SMA(3:1) copolymer (S) and lipid (L) from vesicular bilayers (b) into SMALPs (m). $\Delta G^{b \rightarrow m, o}$ values were calculated from $R_S^{b, SAT}$ and $R_S^{m, SOL}$ with the aid of eqn (3)–(8). 95% confidence intervals are indicated in parentheses below best-fit values.

Lipid	T (°C)	$R_S^{b, SAT}$	$R_S^{m, SOL}$	$\Delta G_S^{b \rightarrow m, o}$	$\Delta G_L^{b \rightarrow m, o}$
DMPC	10	0.039 (0.028–0.047)	0.095 (0.085–0.106)	–1.94 (–2.96–1.38)	0.12 (0.08–0.17)
DMPC	30	0.078 (0.070–0.086)	0.144 (0.134–0.162)	–1.36 (–1.91–1.01)	0.15 (0.11–0.21)
POPC/POPE(1:0)	30	0.108 (0.104–0.113)	0.167 (0.160–0.172)	–0.97 (–1.12–0.77)	0.13 (0.10–0.15)
POPC/POPE(3:1)	30	0.091 (0.086–0.097)	0.192 (0.185–0.198)	–1.66 (–1.85–1.43)	0.22 (0.19–0.25)
POPC/POPE(1:1)	30	0.057 (0.049–0.067)	0.211 (0.203–0.218)	–2.95 (–3.39–2.49)	0.34 (0.30–0.38)
POPC/POPE(1:3)	30	0.065 (0.057–0.074)	0.244 (0.236–0.251)	–2.94 (–3.31–2.57)	0.39 (0.35–0.42)

Supplementary References

- (1) C. Vargas, R. Cuevas Arenas, E. Frotscher, S. Keller, *Nanoscale*, 2015, **7**, 20685.
- (2) D. Lichtenberg, *Biochim. Biophys. Acta*, 1985, **821**, 470.
- (3) G. Kemmer, S. Keller, *Nat. Protoc.*, 2010, **5**, 267.
- (4) M. Roux, P. Champeil, *FEBS Lett.*, 1984, **171**, 169.
- (5) D. Levy, A. Gulik, M. Seigneuret, J. L. Rigaud, *Biochemistry*, 1990, **29**, 9480.
- (6) M. T. Paternostre, M. Roux, J. L. Rigaud, *Biochemistry*, 1988, **27**, 2668.
- (7) T. Heimburg, *Thermal Biophysics of Membranes*, Wiley-VCH: Weinheim, 2007.
- (8) H. Heerklotz, *Q. Rev. Biophys.*, 2008, **41**, 205.
- (9) M. N. Triba, D. E. Warschawski, P. F. Devaux, *Biophys. J.*, 2005, **88**, 1887.
- (10) M. Beaugrand, A. A. Arnold, J. Hénin, D. E. Warschawski, P. T. F. Williamson, I. Marcotte, *Langmuir*, 2014, **30**, 6162.